

Paleoceanography and Paleoclimatology*

RESEARCH ARTICLE

10.1029/2023PA004820

Special Collection:

Illuminating a Warmer World:
Insights from the Paleogene

Key Points:

- At the EECO onset, the abundance of the planktic foraminiferal genera *Morozovella* and *Chiloguembelina* decreased and never recovered
- Species replacement and test-size increase within assemblages sustained production of pelagic carbonate by foraminifera
- Greater adaptability and flexibility of the genus *Acarinina* led to its dominance over the more specialized morozovellids

Supporting Information:

Supporting Information may be found in the online version of this article.

Correspondence to:

G. Filippi,
giulia.filippi@unife.it

Citation:

Filippi, G., Barrett, R., Schmidt, D. N., D'Onofrio, R., Westerhold, T., Brombin, V., & Luciani, V. (2024). Impacts of the early Eocene climatic optimum (EECO, ~53–49 Ma) on planktic foraminiferal resilience. *Paleoceanography and Paleoclimatology*, 39, e2023PA004820. <https://doi.org/10.1029/2023PA004820>

Received 30 NOV 2023

Accepted 27 JUN 2024

Author Contributions:

Conceptualization: Giulia Filippi, Daniela N. Schmidt, Valeria Luciani

Data curation: Giulia Filippi, Ruby Barrett, Roberta D'Onofrio, Thomas Westerhold, Valentina Brombin

Formal analysis: Giulia Filippi, Daniela N. Schmidt








Funding acquisition: Daniela N. Schmidt, Valeria Luciani

Investigation: Giulia Filippi, Valeria Luciani

© 2024. The Author(s).

This is an open access article under the terms of the [Creative Commons Attribution License](#), which permits use, distribution and reproduction in any medium, provided the original work is properly cited.

Impacts of the Early Eocene Climatic Optimum (EECO, ~53–49 Ma) on Planktic Foraminiferal Resilience

Giulia Filippi¹ , Ruby Barrett² , Daniela N. Schmidt² , Roberta D'Onofrio^{1,3} , Thomas Westerhold⁴ , Valentina Brombin¹ , and Valeria Luciani¹ 

¹Department of Physics and Earth Sciences, University of Ferrara, Ferrara, Italy, ²School of Earth Sciences, Cabot Institute, University of Bristol, Bristol, UK, ³CNR, Istituto di Scienze Marine, Venezia, Italy, ⁴MARUM, University of Bremen, Bremen, Germany

Plain Language Summary The Early Eocene Climatic Optimum (EECO) is an interval of prolonged warmth that occurred ~53 to 49 million years ago. Planktic foraminifera are important (alongside coccolithophores) for understanding the carbon cycle and determining export production in the ocean. To understand how foraminifera can be impacted by extreme heat, we analyzed samples from the Pacific Ocean through measuring changes in (a) the relative abundance, that is, the count of different taxa in a sample, and (b) body (shell) size of planktic foraminifera. At the start of the EECO, the abundance of the genera *Morozovella* and *Chiloguembelina* decreased. Despite this decline, the number of foraminifera being buried and the size of the largest shells in a sample does not change. We attribute this to the increased abundance of the genus *Acarinina*. In general, the accumulation of foraminifera remains stable while the relative abundance of foraminifera to coccolithophores decreases. Together, this implies that coccolithophores are increasing in abundance, and/or mass. During the EECO, one group of foraminifera was able to counterbalance the decrease in abundance of other genera. This highlights the resilience of open-ocean carbonate production and the base of the marine food web.

Abstract The Early Eocene Climatic Optimum (EECO; ~53 and 49 Ma) records the warmest long-term global average temperature and highest CO₂ levels of the Cenozoic. Multiple transient global warming events occur within the EECO, offering an opportunity to investigate the impact of extreme heat on planktic foraminifera. Pacific Ocean Drilling Program (ODP) Sites 1209–1210 (Shatsky Rise) provide an excellent age model and stable isotope records to link biotic data with the carbon cycle across the interval here analyzed (55.6 and 49.93 Ma). We combine carbonate production proxies with changes in planktic foraminiferal assemblages and test-size. Our data show that during the EECO planktic foraminiferal assemblages were permanently modified, besides transient changes. At the EECO onset, abundance of the genera *Morozovella* and *Chiloguembelina* decreased at 53.28 and 52.85 Ma, respectively, confirming published Atlantic Ocean data and thus the global decline of these genera. Given the dominance and large size of *Morozovella* in early Eocene tropical assemblages, we postulated that this change would have reduced foraminiferal production and the assemblage test-size. In contrast, we record a slight increase in test-size within assemblages, controlled by the now dominant genus, *Acarinina*. The decrease in coarse fraction weight, partially controlled by dissolution, during times of stable foraminiferal mass accumulation rate indicates enhanced calcareous nannofossil productivity reducing the foraminiferal contribution to the sediment. During the EECO, despite the decrease in abundance of some genera, species replacement within communities highlights the resilience of pelagic carbonate production, emphasizing the critical role of planktic foraminifera in regulating the marine food web and global carbon cycling.

1. Introduction

The Cenozoic Sea surface temperatures attained their warmest long-term state during the Early Eocene Climatic Optimum (EECO; ~53 and 49 Ma) (Hollis et al., 2012; Huber & Caballero, 2011; Inglis et al., 2015, 2020; Zachos et al., 2008) caused by high atmospheric CO₂ levels (e.g., Anagnostou et al., 2016; Hönisch et al., 2023; Zachos et al., 2008). In addition, transient (40–200 kyr) hyperthermals caused by perturbations of the carbon cycle resulted in short-lived warming events (Kirtland-Turner et al., 2014; Littler et al., 2014; Zachos et al., 2005). The global mean surface temperature estimates for the EECO (27.0°C) suggest temperatures ~10–16°C warmer than Holocene (Gaskell et al., 2022; Inglis et al., 2020). This time interval therefore has great potential for exploring

Methodology: Giulia Filippi, Ruby Barrett, Roberta D'Onofrio, Valentina Brombin
Project administration: Valeria Luciani
Supervision: Daniela N. Schmidt, Valeria Luciani
Validation: Daniela N. Schmidt, Valeria Luciani
Visualization: Giulia Filippi, Daniela N. Schmidt, Roberta D'Onofrio
Writing – original draft: Giulia Filippi, Daniela N. Schmidt, Valeria Luciani
Writing – review & editing: Giulia Filippi, Ruby Barrett, Daniela N. Schmidt, Roberta D'Onofrio, Thomas Westerhold, Valentina Brombin, Valeria Luciani

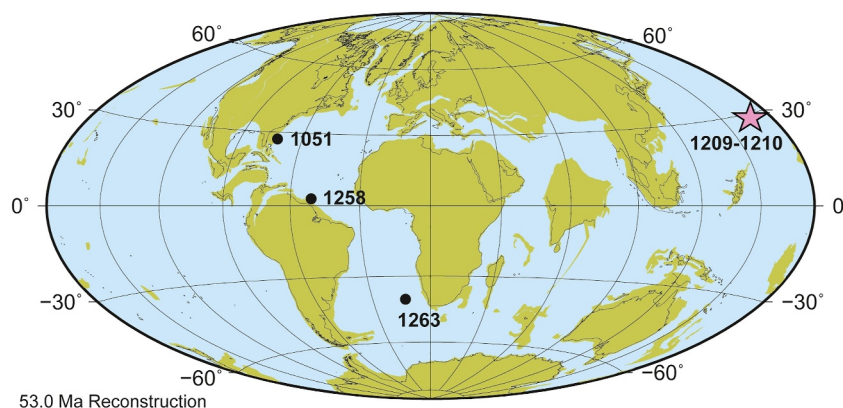


Figure 1. Approximate location of the studied sites 1209 and 1210 during the early Eocene (pink star). Also shown are the locations of Ocean Drilling Program (ODP) Atlantic sites 1051, 1258 and 1263 (black dots), where planktic foraminiferal records show a major change in genera across the EECO and $\delta^{13}\text{C}$ records are detailed (D'Onofrio et al., 2020; Luciani et al., 2017a, 2017b). The base map is from https://www.odsn.de/odsn/services/paleomap/adv_map.html with paleolatitudes modified for sites 1051, 1263, 1258, and 1209–1210 according to www.paleolatitude.org model version 1.2 (Van Hinsbergen et al., 2015). Note that locations might be adjusted to a different reference frame to account for changes in plate motion relative to the spin axis (Hollis et al., 2019).

the marine organism response to extreme warmth through a long-term perspective, which is prevented from studies on modern fauna. Such long-term perspective enables us to explore the resilience of a system. Resilience can be expressed as the ability of a population to resist a disturbance, (e.g., via migration) and/or recover from disturbance (e.g., Capdevila et al., 2020) by returning to a stable state (Hodgson et al., 2015). The ongoing pronounced increase in temperature is compromising ecosystem resilience in modern oceans. The impacts of warming include range shifts due to species migration toward higher latitudes and deeper waters, reductions in growth, reproduction and other physiological processes as well as local extinctions (e.g., Chaabane et al., 2023; Cooley et al., 2022; Raven et al., 2005; Woodhouse et al., 2021).

To understand how marine pelagic carbonate production responds to global warming is crucial due to the key role of planktic foraminifera and calcareous nannoplankton in regulating the marine carbon cycle through the production and subsequent burial of their calcium carbonate exoskeleton (Ridgwell & Zeebe, 2005). In the modern ocean, planktic foraminifera contribute 23%–56% of pelagic carbonate production and 32%–80% of total CaCO_3 flux to the sea floor (Knecht et al., 2023; Neukermans et al., 2023; Schiebel, 2002), though there are significant differences between ocean basins and latitudes, with the highest values recorded in tropical, northern Pacific, Southern Ocean and upwelling regions (Buitenhuis et al., 2013; Schiebel, 2002). The marine carbon sink is generally considered vulnerable to environmental change due to sensitivity to warming (Cooley et al., 2022), however the links between high temperature, ecosystem resilience and carbonate production are insufficiently understood.

During the PETM, nannofossils underwent significant changes, including a major assemblage turnover, reduced abundance and diversity, and a biocalcification crisis, with opportunistic species temporarily prevailing due to severe environmental stress (Agnini et al., 2006; Raffi et al., 2009; Sharman et al., 2023; Wang et al., 2022). These changes continued into the EECO, marking the beginning of a shift toward their modern structure, particularly during the *Toweius-reticulofenestrid* turnover (Agnini et al., 2006, 2009; Cappelli et al., 2019; Gibbs et al., 2012; Schneider et al., 2011). In response to warming, a poleward migration of warm-index taxa is recorded during the EECO (e.g., Alegret et al., 2021).

Among planktic foraminifera, the symbiont-bearing mixed-layer genera, *Morozovella* and *Acarinina*, are important early Paleogene tropical and subtropical taxa (Boersma et al., 1987; Premoli Silva & Boersma, 1988). These genera permanently switched their abundance in the Atlantic Ocean close to the start of the EECO (Figure 1) (D'Onofrio et al., 2020; Luciani et al., 2016, 2017a, 2017b) as *Morozovella* abundance decreased significantly while *Acarinina* increased (Aze et al., 2011; Fraass et al., 2015; Pearson et al., 2006). Similar permanent reductions in abundance are noted for the deeper-dweller genus, *Chilouembelina*, that radiates in the middle Eocene and

ranges up to the Oligocene (e.g., Premec Fucek et al., 2018; King & Wade, 2017; Pearson et al., 2006) but virtually disappears from several latitudes of the Atlantic Ocean within the EECO (Luciani et al., 2020).

As well as abundance, test-size and weight of planktic foraminifera (and dissolution related loss) modulate carbonate burial in sediments (e.g., Ridgwell & Zeebe, 2005). Test-size responds to environmental conditions, which alter physiological performance and species composition (Kucera, 2007). Most modern species reach largest size at their optimal conditions, where food and temperature are advantageous (De Villiers, 2004; Hecht, 1976; Kennett, 1976; Lombard et al., 2009; Schmidt, Renaud, et al., 2004, Schmidt, Thierstein, & Bollmann, 2004, 2006; Spero et al., 1991). In addition, extant low-latitude and symbiont-bearing planktic foraminiferal species are generally larger than those lacking symbiotic relationships as symbiosis plays an important role in calcification, longevity and growth in the oligotrophic mixed-layer (Bé et al., 1982; Caron et al., 1982; Schmidt, Renaud, et al., 2004, Schmidt, Thierstein, & Bollmann, 2004, 2006). Similar differences between taxa are also noted in the early Eocene with *Morozovella* and *Acarinina* having a larger test-size than the asymbiotic *Subbotina* (e.g., Pearson et al., 2006). However, although species diversity in the early Eocene increased to above the Cenozoic average (e.g., Fraass et al., 2015), the generally lower sizes of planktic foraminifera during the early Eocene could be related to the weaker vertical temperature gradient than the late Eocene and afterward, impacting the biological pump and food availability in the upper water column (e.g., John et al., 2013; Schmidt, Thierstein, & Bollmann, 2004).

The aim of our study is to assess the relationship between changes in planktic foraminiferal assemblages during the early Eocene and carbonate production. We will also establish whether the morozovellid and chiloguembelinid decline in abundance across the EECO is recorded outside the Atlantic Ocean. We selected the Ocean Drilling Program (ODP) sites 1209–1210 (Shatsky Rise) that provide common planktic foraminiferal assemblages, a high-resolution age model and stable isotope data across the EECO, thus allowing a comparison of the acquired records with environmental change. We evaluate whether planktic foraminiferal test-sizes and carbonate productivity were influenced by these abundance changes and provide new insights on planktic foraminiferal response to warm climates.

2. Material and Methods

We analyzed pelagic sediment cores of Ocean Drilling Program (ODP) Leg 198, sites 1209 (present water depth = 2,387 m) and 1210 (present water depth = 2,573 m) on Shatsky Rise from the tropical Pacific Ocean (Bralower, Premoli Silva, & Malone, 2002; Westerhold & Röhl, 2006) (Figure 1). Sediments from both sites consist of nannofossil ooze with occasional intervals of nannofossil ooze with clay (Bralower, Premoli Silva, & Malone, 2002, Bralower, Premoli Silva, Malone, et al., 2002). Fossil preservation is sufficiently good for assemblage studies and enables reliable taxa identification (Bralower, Premoli Silva, & Malone, 2002).

We adopt the age model and meter composite depth of Westerhold et al. (2018). We analyzed 73 samples from Site 1209 (Holes A and B), covering an age interval from 53.14 to 49.93 Ma (Westerhold et al., 2018) and spanning from Hole B Core 21H 187.62 mbsf (meters below sea floor), that is, 208.16 rmcd (revised composite depth) to Hole B Core 19H 172.50 mbsf, that is, 189.70 rmcd (Table S2 in Supporting Information S1). The older part of the record was analyzed at Site 1210 with an overlap of ~1 Myr. We selected 66 samples from Site 1210 (Holes A and B) covering a time interval between 55.60 and 52.26 Ma (Westerhold et al., 2018) and spanning from Hole A Core 20H 183.640 mbsf, that is, 206.425 adj rmcd (adjusted rmcd accounting for samples outside the defined composite), to Hole A Core 19H 170.73 mbsf, that is, 192.440 adj rmcd (Table S3 in Supporting Information S1). The sampling spacing is ~0.10 m across the hyperthermals rmcd and ~0.40 m between the hyperthermals for both the sites resulting in a resolution of ~20 and ~200 kyr respectively (Tables S2 and S3 in Supporting Information S1).

2.1. Stable Isotope Analysis

Isotope data for Site 1209 were generated on benthic foraminifera *Nuttallides truempyi* and *Oridorsalis umbonatus* by Westerhold et al. (2018). Carbon and oxygen stable isotopes from Site 1210 were performed on bulk sediments at the Stable Isotope Laboratory of the Department of Geosciences at the University of Padova using a Thermo Scientific Delta V Advantage Isotope Ratio Mass Spectrometer coupled with a Gas Bench II automated preparation device on bulk samples. Samples were first freeze-dried and then pulverized manually with a mortar. Samples of ~200–250 µg were flushed with helium and then treated with 10 mL of 100% phosphoric acid

(EMSURE® ≥ 99%) at 70°C for ca. 3 hr. Isotopic values are reported in standard delta notation relative to the Vienna Pee Dee Belemnite (VPDB). During the analyses an internal standard (white Carrara marble Maq 1: δ¹³C = +2.58‰; δ¹⁸O = −1.15‰ VPDB) was used to normalize raw δ¹³C and δ¹⁸O values and a check standard (marble Gr1: δ¹³C = +0.68‰; δ¹⁸O = −10.44‰ VPDB) was run for quality assurance, and repeated with precisions better than 0.07‰ for δ¹³C, and better than 0.09‰ for δ¹⁸O. Raw data are shown in Tables S2 and S3 in Supporting Information S1.

2.2. Proxy for Carbonate Production and Dissolution: Fragmentation Index, CF and FMAR

Deep sea carbonate dissolution, commonly associated with early Eocene negative carbonate isotope excursions (CIEs) causes planktic foraminifera to break into fragments (e.g., Berger, 1970; Hancock & Dickens, 2005; Nguyen & Speijer, 2014). Genera/species specific dissolution susceptibility could therefore bias the assemblage record (e.g., Nguyen et al., 2009, 2011; Petrizzo et al., 2008). We adopt the fragmentation index (F index) as a dissolution proxy (Berger, 1970) which is the ratio between fragments or partially dissolved planktic foraminiferal tests versus entire tests on ~300 individuals >63 μm, and expressed as percentage (Tables S2 and S3 in Supporting Information S1).

The ratio between coarse fraction ≥38 μm and the bulk dry sediment was calculated following Hancock and Dickens (2005) as weight percent coarse fraction (CF). The CF is a second dissolution proxy that can also give information about planktic foraminiferal productivity when pelagic sediments are not affected by dissolution (Hancock & Dickens, 2005) (Tables S2 and S3 in Supporting Information S1).

We evaluated the Foraminiferal Mass Accumulation Rate (FMAR; Equation 1) to determine whether changes in coarse fraction percentages, in time intervals not affected by great carbonate dissolution, were driven by changes in the abundance of foraminifera or by fluctuations in nannofossil productivity.

$$\text{FMAR} = \frac{(\text{Carbonate Accumulation} \times \text{Coarse Fraction } \%) }{100} \quad (1)$$

The carbonate accumulation (g/cm²/kyr; Equation 2) is a function of bulk accumulation (g/cm²/kyr) and carbonate percent (% CaCO₃; Bralower, Premoli Silva, & Malone, 2002; Coffin et al., 2000; Norris et al., 2014).

$$\text{Carbonate accumulation} = \text{bulk accumulation} \times \% \text{CaCO}_3 \quad (2)$$

Bulk accumulation (g/cm²/kyr) is calculated from the linear Sedimentation Rate (SR; cm/kyr) and Dry Bulk Density (DBD; g/cm³). The %CaCO₃, SR at site 1210, as DBD are following Bralower, Premoli Silva, and Malone (2002). SR dropped from ~6 to 2 m/my between 57 and 53 Ma at Site 1210, SR at Site 1209 is adjusted by Westerhold et al. (2018). The relationship among data on preservation, FMAR and CF can help to discriminate the drivers of carbonate sedimentation.

2.3. Planktic Foraminiferal Analysis

Bulk samples were oven-dried at 45°C, weighed, and then immersed in deionized water.

Disaggregation occurred from a few hours to 3 days, depending on the compactness of the sediments. When disaggregated, samples were washed over stacked ≥63 and ≥38 μm sieves. After each wash, sieves were immersed in a methylene blue bath to assess contamination (e.g., Green, 2001). The separated fractions of each washed residue were dried at 45°C.

Planktic foraminifera were studied from washed residues (≥63 μm fraction) using a Zeiss stereomicroscope and presence/absence of zonal markers established (Table S1, Text S1 in Supporting Information S1). The taxonomic criteria adopted to identify planktic foraminiferal genera and species follow Olsson et al. (1999) and Pearson et al. (2006). The main early Eocene planktic foraminiferal biohorizons (Wade et al., 2011) can be identified at Site 1209–1210. However, cases of diachronism were recorded concerning the standard scheme by Wade et al. (2011) in agreement with Luciani and Giusberti (2014), D'Onofrio et al. (2020), Luciani et al. (2017a, 2017b). Relative abundances of planktic foraminiferal genera were determined on more than 300 specimens of the ≥63 μm size fraction from random splits generated by a microsplitter. Foraminiferal relative abundance quantitative data are provided in Tables S4 and S5 in Supporting Information S1. In the genus *Subbotina* we do not

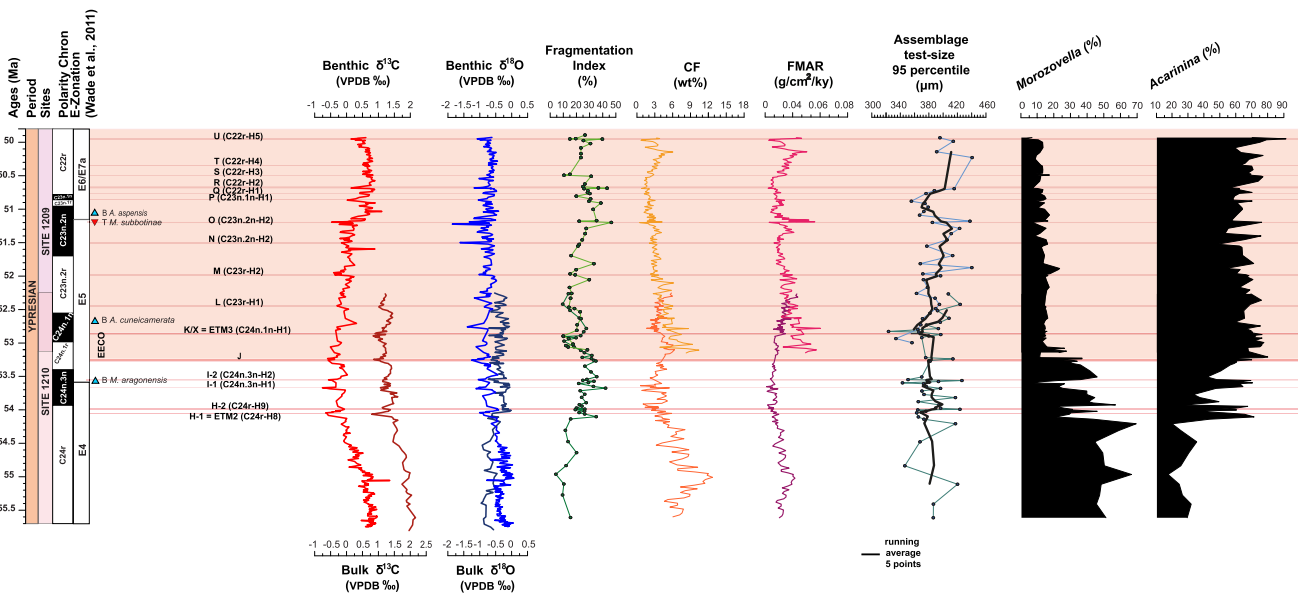


Figure 2. Stable isotope records at ODP sites 1209 and 1210 along with Fragmentation index (%), weight percent coarse fraction (CF), Foraminiferal Mass Accumulation Rate (FMAR) and test size 95th percentile (μm) plotted in age (Ma; according to the age model of Westerhold et al., 2018). The dark red bulk $\delta^{13}\text{C}$ and dark blue bulk $\delta^{18}\text{O}$ and curves are from this work and referred to Site 1210. The benthic foraminifera red and blue curves are from Westerhold et al. (2018) and referred to Site 1209. The abundances (%) of the genera *Morozovella* and *Acarinina* that show marked changes across the interval investigated are also reported. The planktic foraminiferal E-zonation follows Wade et al. (2011) as partly modified by Luciani and Giusberti (2014). The main calcareous nannofossil horizons are also reported according to Bralower et al. (2005) and adapted to the Agnini et al. (2014) zonal scheme. Main carbon isotope excursions (CIEs) are labeled according to Westerhold et al. (2017). We separate Site 1210 from site 1209 with darker shade of color with respect to Site 1209 (e.g., 1209 Fragmentation Index is light green, 1210 Fragmentation Index is in dark green).

include the species *Subbotina senni* as *S. senni* was a mixed-layer species that migrated to middle mixed-layer or deeper depths during gametogenesis, meaning it presents a different ecology with respect to the subbotinids groups (Pearson et al., 1993, 2006). In the subbotinids group we include rare *Parasubbotina* specimens (*P. inaequispira*, *P. varianta*) as these species are known as having a thermocline habitat similar to *Subbotina* (e.g., Pearson et al., 2006, and references therein).

In addition, we assessed the variation in test-size for the entire assemblage in 77 samples distributed from 208.16 to 189.70 rmcd (Site 1209), and in 42 samples from 192.440 to 201.790 adj rmcd (Site 1210) following the method in Schmidt, Renaud, et al. (2004). Samples $>150 \mu\text{m}$ were split using a microsampler to aliquots from a minimum of 818 to a maximum of 3,541, with an average of 1759 specimens per sample. These were imaged at $160\times$ magnification and the morphological parameters of each specimen were analyzed in Olympus Stream Motion. To remove juvenile specimens and lithic fragments from analyses, the morphological parameters were set to exclude particles with a diameter $<150 \mu\text{m}$, sphericity <0.5 and gray value below 80. Benthic foraminifera and ostracods were removed via manual assessment. The 95th percentile of the maximum diameter of all foraminiferal in the assemblage was calculated (Schmidt, Renaud, et al., 2004).

3. Results

3.1. Stable Isotopes, F Index, CF, and FMAR

The $\delta^{13}\text{C}$ values across Site 1210 vary between ~ 0.79 and $\sim 2.16\%$, with an average of 1.35% (Figure 2, Tables S2 and S3 in Supporting Information S1) and a general decreasing trend with time. The $\delta^{18}\text{O}$ values at Site 1210 range between -0.96% and -0.02% , with a mean value of -0.42% (Table 1, Figure 2). The relationship with CIEs and hyperthermals is according to Westerhold et al. (2018) (Table 1, Figure 2).

The F index shows a mean value of $\sim 23\%$ with a minimum of $\sim 10\%$ and a maximum of 46% for the whole interval investigated at both sites (Figure 2, Table 1, Tables S2 and S3 in Supporting Information S1). High, above average values, are associated only with selected CIEs (e.g., H1, I1, J, O, P, Q, R, S and U). The lower values are recorded

Table 1
Relationship Among Fragmentation Index and Main CIEs at Shatsky Rise

Age ^a (Ma)	Depth ^b (rmcd)	CIEs ^c	$\delta^{13}\text{C}^{\text{d}}$ (%)	$\delta^{18}\text{O}^{\text{e}}$ (%)	F index ^f (%)
Site 1209					
49.95	189.90	U (C22rH5)	0.13	-1.09	40
50.35	192.55	T (C22rH4)	0.56	-0.67	20
50.49	193.60	S (C22rH3)	0.83	-0.79	26
50.68	194.63	R (C22rH2)	0.14	-1.18	43
50.76	195.20	Q (C22rH1)	0.41	-0.90	30
50.86	195.70	P (C23n.1nH1)	0.45	-0.65	30
51.23	198.17	O (C23n.2nH2)	-0.24	-1.87	45
51.55	199.99	N (C23n.2nH1)	0.07	-0.59	21
51.98	202.07	M (C23rH2)	-0.37	-1.03	19
52.46	204.67	L (C23rH1)	-0.18	-0.87	14
52.86	206.85	K/X (C24n.1nH1)			20
Site 1210					
52.84	195.140	K/X (C24n.1nH1)	0.95	-0.36	26
53.26	197.360	J (C24n.2rH1)	1.06	-0.65	34
53.56	198.960	I2 (C24n.3nH2)	1.15	-0.73	25
53.67	199.570	I1 (C24n.3nH1)	1.31	-0.36	42
53.99	201.192	H2 (C24rH9)	1.38	-0.2	20
54.05	201.530	H1/ETM2 (C24rH8)	1.08	-0.64	22

Note. Age (Ma)^a and depth (rmcd, adj rmcd)^b of the main CIEs^c from Westerhold et al. (2017) as identified from the minimum values of $\delta^{13}\text{C}^{\text{d}}$ and $\delta^{18}\text{O}^{\text{e}}$ (benthic foraminifera) at ODP Site 1209 (Westerhold et al., 2018) and bulk at Site 1210, along with the values of Fragmentation index (%)^f estimated in the corresponding samples.

at Site 1210 below the ETM2 CIE (mean value ~16%). The interval between the ETM2 and J events display an increase (mean value of ~27%), that is also associated with CIEs. After this increase, fragmentation decreases below the K/X event at Site 1209 (mean value ~16%) then increases again until the L event (mean value of ~22%). A slight increase is registered starting from the K/X CIE up the top of Site 1209 as the F index mean value is of ~27%.

With the exception of an increase between 53.27 Ma and 52.86 Ma, and a slight increase between ~53.70 and ~53.10 Ma, CF decreases from 55.01 Ma toward the top of the recorded succession, as previously observed in Bhattacharya and Dickens (2020) and Hancock and Dickens (2005) Higher values generally correspond to the CIEs (Figure 2, Tables S2, S3, Text S2, Figure S1 in Supporting Information S1). The lowest CF contribution to the sediment before the EECO records 0.6% (53.64 Ma), and 0.4% during the EECO (51.19 Ma, above O CIE), and the highest contribution is 13% (55.01 Ma).

The FMAR shows a mean value of ~0.02 g/cm²/kyr, a minimum value of 0.002 g/cm²/kyr, and the highest value of 0.062 g/cm²/kyr after 52.86 Ma (K/X Event). After the K/X CIE, long-term relatively stable values are noted over time (~0.023 g/cm²/kyr; Figure 2, Tables S2 and S3 in Supporting Information S1).

3.2. Variations in Abundance of Planktic Foraminiferal Taxa

The early Eocene planktic foraminiferal assemblages exhibit both long-term and transient changes throughout the studied interval (Figure 3, Tables S4 and S5 in Supporting Information S1). The most significant changes involve the abundances of dominant mixed-layer dwelling warm-index taxa, acarininids and morozovellids. *Morozovella* records a general decreasing trend starting with a mean value of ~51% below the ETM2 CIE, then moving to ~33% from ETM2 to J CIEs and markedly decreasing with a mean value of ~14% from the EECO onset until the top of the interval. In contrast, the abundance of *Acarinina* increases from ~31% in the pre-ETM2 to ~52%

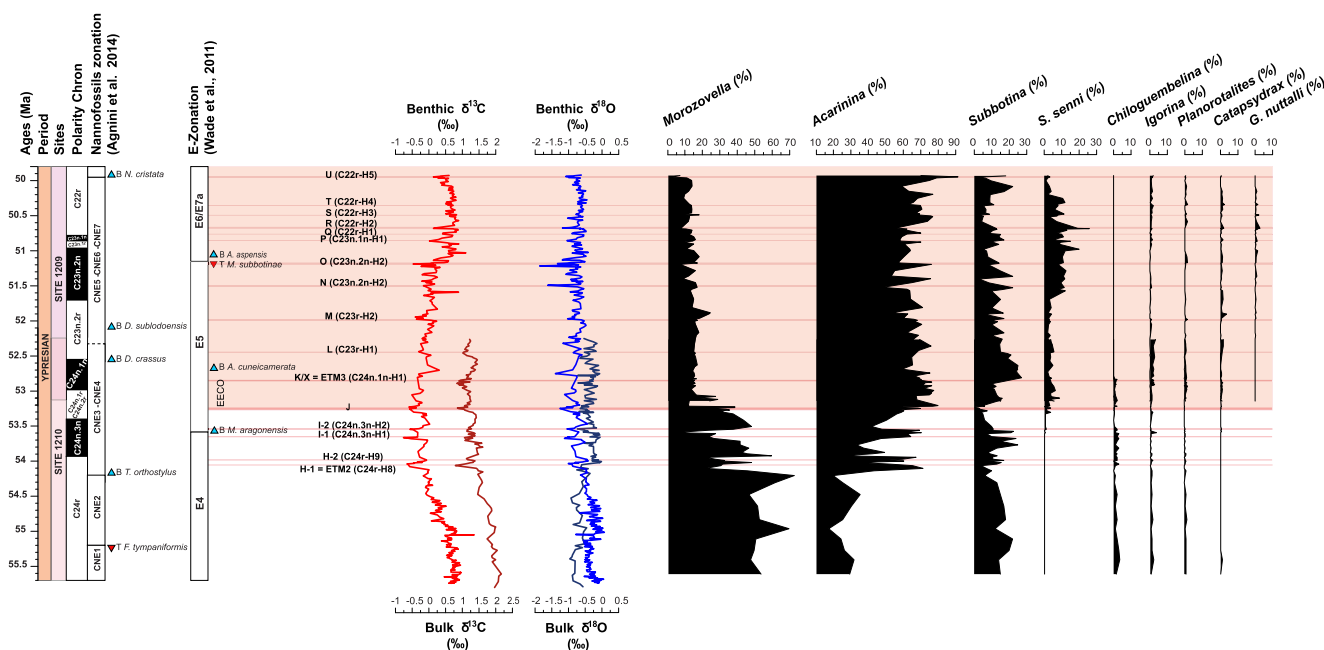


Figure 3. Relative abundances of planktic foraminiferal taxa across the early Eocene interval at ODP sites 1210 and 1209. The genus *Subbotina* includes *Parasubbotina*. Note the major switch in *Morozovella* and *Acarinina* abundances at the J event and the virtual disappearance of *Chiloguembelina* above the K/X event. Other information is consistent with Figure 2.

between the ETM2 and J CIEs to reach a mean value of ~66% above the EECO onset. The ANOVA performed on morozovellids and acarininids comparing their mean value in abundance in pre-ETM2, ETM2-J, Post-J intervals confirms that there are differences in abundance between intervals (p value < 0.05). Before the CIE corresponding to the J Event, subbotinids record an average relative abundance of ~11%. A short-term increase is registered starting from the J until the L CIEs, with maximum value of 27% at 52.80 Ma. A long-term slight reduction in subbotinid abundance occurs in the EECO after the L event (52.86 Ma) (mean value ~11%).

On shorter timescales, fluctuations in the abundance of *Acarinina* are in antiphase with *Morozovella* and subbotinids abundances. This is particularly evident across the CIEs. Acarininids appear to be able to acclimatize to the conditions associated with these CIEs best as indicated by their high abundances, though the abundances of morozovellids and subbotinids often recover rapidly above the CIEs (Figure 3). However, it is important to acknowledge that the observed changes in abundances mentioned above are relative and therefore influenced by a closed-sum effect, meaning that a decrease in one genus corresponds to an increase in one or more other genera. In addition, there is an offset in abundance between the morozovellids and subbotinid records of Site 1209 with respect to Site 1210. These differences might be attributed primarily to spatial and deposition factors, as the sites are about 50 km apart on a gradual slope, as well as to sampling processing, bioturbation, and sediment mixing. Both sites are correlated to each other with high confidence according to Westerhold et al. (2018) (see Figure S6 in Supporting Information S1) and thus the age model does not contribute to the offsets in the data between sites.

A significant drop in relative abundance of the genus *Chiloguembelina* occurs during the EECO. Abundance decreases from a mean value of ~10% to virtually absent and does not recover during the analyzed time interval (Figure 3, Tables S4 and S5 in Supporting Information S1). We carefully checked also the fraction $\geq 38 \mu\text{m}$ as this genus has a small, narrow test that could bypass the $63 \mu\text{m}$ sieve. Results confirm its absence as recorded by the analysis of the $\geq 63 \mu\text{m}$ fraction. The species *Subbotina senni* shows abundance increase from the 3.72% up to ~9.15% in the upper part of the succession. The genera *Igorina*, *Planorotalites*, *Globanomalina*, *Catapsydrax* and the species *Guembeltriodes nuttalli* are very rare in the assemblages throughout the early Eocene and never exceed 5% in terms of total planktic foraminifera abundance. These forms show little variability throughout the investigated interval.

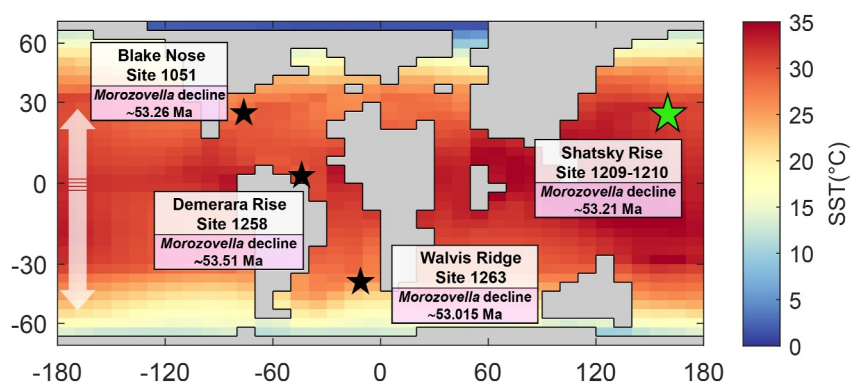


Figure 4. Site locations of ODP sites 1209–1210 (green star), 1051, 1258 and 1263 (black stars) showing the age (Ma) of the *Morozovella* decline in abundance as recorded by this work, Luciani et al. (2017a, 2017b) and D’Onofrio et al. (2020) respectively. Sea surface temperature (SST) output is modeled by ForamEcoGENIE and is a steady state early Eocene spin-up (Wilson et al., 2018). The white arrow is to note that the observed decline in *Morozovella* abundance originated in the Atlantic equatorial location and then expanded to mid-latitudes.

3.3. Variations in Test-Size of Planktic Foraminiferal Taxa

Test-size 95th percentile ranges between 323 and 426 μm with an average value of 384 μm (Figure 2, Tables S4 and S5 in Supporting Information S1). Higher test-size generally corresponds to *Acarinina* abundance peaks across the CIEs and to high morozovellid abundance before the onset of the EECO. Size increases from the K/X CIE (52.86 Ma), coincides with the highest abundance of acarininids (Figure 2).

4. Discussion

Our data show clear links between changes in taxa composition and carbonate production across the studied interval. Associated with the onset of the EECO, the composition of foraminiferal assemblages changed markedly and did not return to pre-event composition during the whole interval analyzed, and even in the post-EECO when temperatures cooled (e.g., Fraass et al., 2015; Luciani et al., 2017a; Swain et al., 2024). Our data, combined with information in the literature, shows that the marked drop in abundance of morozovellid and chiloguembelinid is a signal recorded in the Pacific Ocean, as well as the Atlantic and Tethys (Luciani et al., 2016, 2017a, 2017b; D’Onofrio et al., 2020), thus it is possibly global. Our data also shows that the genus *Acarinina* was less affected from the environmental change as change in abundance within communities sustained overall test-size and the production of pelagic carbonate by foraminifera (Figures 2 and 3). The evolutionary replacement of species with larger test-size may have also contributed to this record. We will explore the reasons for *Acarinina*’s greater adaptability and flexibility that led to its dominance across the EECO compared to the more specialized morozovellids, and causes for the chiloguembelinids virtual disappearance.

4.1. Resilience and Vulnerability of Planktic Foraminiferal Genera in a Geographic and Temporal Context

Our results highlight that the genus *Morozovella* markedly decreased in abundance, unable to tolerate the environmental changes associate with the EECO. In contrast, *Acarinina* was a “winner” as it exhibited greater ecological adaptability, allowing this genus to thrive. This latter genus benefitted from the temperature rise at the pre-EECO and EECO hyperthermals, as shown by the increase in *Acarinina* abundance with respect to *Morozovella* (e.g., D’Onofrio et al., 2020; Luciani et al., 2016, 2017a, 2017b; this paper Figure 2).

The decrease in *Morozovella* and increase in *Acarinina* did not happen simultaneously at all sites (Figure 4), in contrast to the *Chiloguembelina* disappearance that starts close to ~ 53.8 Ma (K/X Event) in both the Atlantic and Pacific Oceans. According to the adopted age model by Westerhold et al. (2018), the switch in abundances of *Morozovella* and *Acarinina* at Site 1258 occurs at 53.51 Ma, ~ 25 kyr before the onset of the EECO (Demerara Rise, D’Onofrio et al., 2020). At the subtropical Atlantic Site 1051 (Blake Nose; Luciani et al., 2017a) the timing of the *Morozovella* decrease at ~ 53.26 , coincides with our new Pacific data at ~ 53.21 Ma, close to the J event. The record at 1210 is more complete as the J event is not recorded at Site 1209. Therefore, the increase in

abundance at Site 1209 above the J event may have been a temporary fluctuations after a decline, which likely occurred previously and synchronously with Site 1210. For these reasons the timing of abrupt *Morozovella* decline in this study is selected at 53.21 Ma. In contrast, in the temperate South Atlantic Site 1263 the genus was able to persist longer with a decline ~25 kyr after the J event (Walvis Ridge; Luciani et al., 2017b) (Figure 4).

The mechanisms and triggers driving the *Morozovella-Acarinina* shift in abundance remain elusive. The timing, starting in the equatorial setting and later in mid latitudes, suggest that a maximum temperature tolerance for *Morozovella* was reached earlier in warmer settings (e.g., Zachos et al., 2003). Nevertheless, to establish the precise role of warming, we need a paleotemperature record across the sites where planktic foraminiferal changes are documented. Following the hypothesis that the decline of morozovellids is related to the effect of the EECO warming, it can appear incongruous that morozovellids increased in abundance from Shatsky Rise rather than declining at the PETM (Petrizzo, 2007) when temperatures were even higher than those at the EECO (e.g., Inglis et al., 2020). A possible explanation of this different behavior may be found in diverse species composition of *Morozovella* across the two time intervals, with the PETM dominated by *M. velascoensis* which went extinct at the base of the earliest Eocene Zone E3 (Wade et al., 2011), well before the EECO interval. Interestingly, Pearson et al. (1993) documents a dominant sinistral coiling of the *Morozovella velascoensis* group during the PETM. We speculate that sinistrally coiled forms are a cryptic species that had a greater tolerance to the warming, as also suggested by the dominance of sinistral forms at the EECO (Luciani et al., 2021). The species *M. aequa*, *M. crater*, *M. lensiformis*, and *M. subbotinae* appear to have persisted in the cooler higher latitudes, where they are the most abundant forms (D'Onofrio et al., 2020). The southern high latitudes may have therefore provided refugia from extreme warming (Swain et al., 2024), but for no more than a limited period of ~270 kyrs. This timing is determined by the different ages of the morozovellid decline across latitudes (Figure 4).

The genus *Chiloguembelina* was also strongly impacted as it permanently disappears ~50 kyr after the K/X Event (52.86 Ma) at Shasky Rise, as already recorded in the Atlantic Ocean (Luciani et al., 2020). As the EECO was characterized by several CIEs that may have induced upward shift of the lysocline/CCD, we could infer that the absence of chiloguembelinids from the deep-water sites analyzed here may be an artifact of dissolution. Chiloguembelinids have thin/small tests that make them more prone to dissolution than taxa with larger thicker/tests (e.g., Nguyen et al., 2011). However, we can exclude that the decline in abundance of chiloguembelinids derives from taphonomic bias because they are very rare or absent above the K/X CIE and from the intervals where the dissolution proxy F-index is very low (Figure 2). The biology and distribution of biserial foraminifera characterize them as low-oxygen tolerant, meso-to eutrophic thermocline dwellers, which thrive in stressed environmental conditions (e.g., Boersma & Premoli Silva, 1989). However, this ecological interpretation does not agree with all Cenozoic records that sometimes ascribe them as surface-water dwellers (e.g., Barrera and Huber, 1991; D'Haenens et al., 2012; Premec Fucek et al., 2018). Nevertheless, Luciani et al. (2020) demonstrate that on the basis of the stable isotope signature of *Chiloguembelina* being close to subbotinids, that during the early Eocene, *Chiloguembelina* inhabited a thermocline environment, except for at high-latitude waters where it migrated to the mixed layer (e.g., Kroon & Nederbragt, 1990; Leckie, 1987; Nederbragt, 1991). We hypothesize, following Luciani et al. (2020), that a contraction of the Oxygen Minimum Zone (OMZ) may have impacted the chiloguembelinid niche. This is supported by Foraminiferal Bound- $\delta^{15}\text{N}$ which suggests low water-column denitrification in eastern tropical North Pacific during the EECO (Auderset et al., 2022). The observed low water-column denitrification may be linked to a decrease in biological productivity in the tropical Pacific during the EECO. This decrease in productivity is attributed to increasing stratification at high temperatures. The stratification is thought to reduce the demand for oxygen in subsurface waters (Auderset et al., 2022). This interpretation is supported by a later occurrence of chiloguembelinids in the late Oligocene in the Pacific Ocean which has been related to the expansion of the Oxygen Depleted Zone (ODZ) (King & Wade, 2017). In addition, elevated ocean temperatures enhanced bacterial respiration thus resulting in more efficient recycling of nutrients higher in the water column (John et al., 2013, 2014; Pearson & Coxall, 2014) and reduced food supply in the thermocline. The eutrophic cold-index *Subbotina* does not display a significant reduction at Shatsky Rise despite a similar habitat and need for food supply. Although the genus *Subbotina* moved to a shallower habitat during the Middle Eocene Climatic Optimum (Kearns et al., 2021), stable isotope data from the Atlantic Ocean support a thermocline niche for this genus across the EECO (Luciani et al., 2020). Therefore, a combination of higher temperatures and reduction of food supply may have contributed to the disappearance of chiloguembelinids during the EECO.

Among the minor component of the assemblages, the increase in abundance of *Subbotina senni* at the start of the EECO is in agreement with the Atlantic sites 1258 and 1263 (D'Onofrio et al., 2020; Luciani et al., 2017b). It is

unlikely that the increase of this species counter-balanced the decrease in subbotinids in terms of ecological replacement, because the former taxon occupied a different habitat (Pearson et al., 1993, 2006 and references therein). It is instead possible that this species, considered as a mixed-layer form that sank to the middle mixed-layer or deeper depths during gametogenesis (above references), might have partly occupied the ecological niches released by morozovellids and/or chiloguembelinids in the Atlantic and Pacific Oceans. The relative abundance of *Igorina* and *Planorotalites* is slightly higher at the Atlantic Site 1258 with respect to Site 1209, suggesting the preference of these genera to an equatorial setting. The occurrence of *Guembelitroides nuttalli* at Site 1209, though rare, is well below its putative first appearance at the base of the middle Eocene Zone E8. This is in good agreement with the record from the Tethyan Possagno section and Atlantic Ocean (D'Onofrio et al., 2020; Luciani & Giusberti, 2014; Luciani et al., 2016, 2017b) and confirms the need for a biostratigraphic review of the zonal scheme by Wade et al. (2011). According to Luciani and Giusberti (2014) the common occurrence of *G. nuttalli* rather than its first appearance, can be the new datum to identify the base of Zone E8 (Text S1, Table S1 in Supporting Information S1).

4.2. *Morozovella* and *Acarinina* Differential Adaptability

We explore potential scenarios to explain the observed *Morozovella* and *Acarinina* switch in abundance. *Morozovella* and *Acarinina* are assumed to have shared the same mixed-layer habitat due to their similar stable isotope values (e.g., Davis et al., 2022; Pearson et al., 2006; Sexton et al., 2006; Shackleton et al., 1985). However, a diverging ecological sensitivity of the two genera is indicated by anti-phase variations across the CIEs, whereby *Morozovella* abundance dropped while *Acarinina* increased (Figures 2 and 3). However, the data needs to be interpreted with caution as morozovellids had a greater sensitivity to dissolution than acarininids (Nguyen et al., 2009, 2011; Petrizzo et al., 2008; Thunell & Honjo, 1981) and hence preservation could have partly controlled the observed response given significant dissolution of up to 30% during the mains CIEs (Table 1). Yet as our findings are supported by other records in different settings during the early Eocene hyperthermal events, even when preservation is much better, (e.g., Agnini et al., 2009; D'Onofrio et al., 2016, 2020; Luciani et al., 2007, 2016, 2017a, 2017b) we have confidence that the original ecological response is at least partially preserved. We deduce that the short-term anti-phase variations across the CIEs reveal different abilities to withstand extreme warmth and the associated change to stratification and food availability. We hypothesize that the prolonged warm conditions during the EECO prevented many species of the genus *Morozovella* from recovering their abundance, in contrast to their response to the short-lived warming during the pre-EECO CIEs.

Symbiosis plays an important role in planktic foraminiferal success, including calcification, longevity and growth, and allows the host to succeed in the oligotrophic mixed-layer. Hence photosymbiont loss (bleaching) may cause population reduction (e.g., Bé et al., 1982; Caron et al., 1982). High temperature is considered the main factor inducing bleaching in recent benthic foraminifera (e.g., Hallock, 2000). The lack of $\delta^{13}\text{C}$ data across tests of different sizes for morozovellids and acarininids from our sections, which determines the presence or absence of photosymbiosis (e.g., Spero & DeNiro, 1987), prevents us from verifying the hypothesis of morozovellid bleaching across the EECO at this sites 1209–1210. Shaw et al. (2021) observed a minor reduction in test-size $\delta^{13}\text{C}$ for *Acarinina soldadoensis* during the PETM at Site 1209, but not for *Morozovella subbotinae*, whereas Davis et al. (2022) did not observe any $\delta^{13}\text{C}$ -derived photosymbiosis activity reduction across Site 1209 ETM2/H2. In addition, transient (~100 kyr) bleaching episodes involving *Acarinina* have been detected at the temperature peak of the Middle Eocene Climatic Optimum (Edgar et al., 2013) and during the EECO in the subtropical Atlantic Site 1051 (Luciani et al., 2017a). It is important to note that differently to the EECO, during the extreme warmth of the PETM the abundance of morozovellids at Shatsky Rise (and elsewhere) markedly increased (Petrizzo, 2007; Shaw et al., 2021).

Interestingly, in addition to the drop in abundance Luciani et al. (2021) showed a change in morozovellid coiling direction from predominantly dextral to prevailing sinistral during the EECO in the Atlantic Ocean. This was interpreted as a change in the abundance of cryptic species which, supported by the lower $\delta^{13}\text{C}$ data recorded by sinistral forms, suggest that this cryptic taxon was less dependent on their photosymbiotic relationship and/or that they moved deeper in the mixed-layer.

Preliminary data from Shatsky Rise, not yet published in full (Filippi et al., 2023), reveal the same change in coiling direction and by analogy the possible selection of a novel cryptic taxon with a slightly different ecology. Davis et al. (2022), testing the photosymbiosis relationships of *Morozovella subbotinae* and *Acarinina*

soldadoensis at the PETM as compared with those of the subsequential minor hyperthermals H1 and ETM2 from Shatsky Rise, record the absence of bleaching during the less extreme warm conditions, differently of a bleaching recorded by the latter species at the PETM, but not affecting the former species. The authors hypothesized that *Acarinina soldadoensis*, and perhaps other acarininids, changed their symbiotic associations in response to the extreme warming of the PETM allowing the long-term evolutionary success of the taxon. This hypothesis appears in line with evidence of greater ecological adaptability in acarininids compared to morozovellids across the EECO. However, the evidence that *Morozovella subbotinae* maintained its photosymbiotic relationship during the relatively warmer PETM may cast doubt on the hypothesis that reduced symbiosis in morozovellids explained their permanent drop in abundance across the EECO. A minor migration down to the mixed layer can also explain the lower $\delta^{13}\text{C}$ values recorded by the sinistral surviving forms after the K/X CIE (Luciani et al., 2021). The contrasting response of morozovellids recorded at multiple PETM sites has been related, besides to different geological settings, to possible variations in photosymbiotic associations (i.e., changes in photosymbiont load, activity, effect, or type of microalgae), though this is poorly constrained in the fossil record (Shaw et al., 2021). We cannot exclude that a reduced efficiency of photosymbiosis started at the PETM and may explain the diverse response of morozovellids during the EECO.

The fossil record does not allow us to explore whether *Morozovella* needed less food than *Acarinina*. Surface-water eutrophication in several Tethyan successions near continental margins have been considered as a feature to explain the high *Acarinina* abundances through the PETM, ETM2, and K/X events (Arenillas et al., 1999; Agnini et al., 2009; D'Onofrio et al., 2016; Ernst et al., 2006; Guasti & Speijer, 2007; Luciani et al., 2007, 2016; Molina et al., 1999). Even though diverse species of *Acarinina* with potentially different ecological preferences may have occurred in the Tethyan realm with respect to the tropical Pacific, in the open ocean conditions at Shatsky rise lower productivity is expected, as supported by the nitrogen isotopes (Auderset et al., 2022). Therefore, there is no supporting evidence, such as the terrigenous input documented for Site 1051, to suggest increased eutrophication coinciding with the recorded decline of morozovellids at Shatsky Rise sites (Bhattacharya & Dickens, 2020; D'Onofrio et al., 2020; Luciani et al., 2016, 2017a, 2017b, this study).

4.3. Disentangling the Impact of the EECO on Planktic Foraminiferal Productivity

One of our aims was to assess how a change in assemblage composition impacted test-size within the assemblage and carbonate production.

The coarse fraction contribution is a product of dissolution, the size of individual taxa, and the productivity of foraminifers and coccolithophores. We do not aim to resolve the full spectrum of drivers of foraminifer accumulation, for example, their weight (Barrett et al., 2023).

Increased dissolution across the CIEs could have caused the lower CF and FMAR (Table 1), for example, during the generally lower CF and FMAR recorded from the ETM2 to J Events (Figure 2 and Bhattacharya & Dickens, 2020; Westerhold et al., 2018).

Interestingly, CF decreases from ~52.86 Ma up to the top of the interval investigated, a trend not recorded in the FMAR (Figure 2). A decrease in CF whilst foraminiferal accumulation remains stable implies a higher calcareous nannofossil contribution to carbonate accumulation (Bhattacharya & Dickens, 2020; Hancock & Dickens, 2005; Westerhold et al., 2018). Relatively high nannofossil productivity during the interval is also supported by the significant increase in carbonate Mass Accumulation Rate (MAR) (see Figure 12 in Bhattacharya & Dickens, 2020; Hancock & Dickens, 2005; Westerhold et al., 2018). This increase is not evident in our FMAR curve because the formula here adopted includes the CF ($\geq 38 \mu\text{m}$ fraction) thus the calcareous nannofossil contribution to the carbonate sediments is hidden, different to the calculation of MAR that accounts for all the carbonate components (Bhattacharya & Dickens, 2020). A partially enhanced foraminiferal dissolution across the interval may have also influenced the relatively low CF values as coccolithophores are more dissolution resistant (Chiu & Broecker, 2008). The increased carbonate dissolution across the EECO is widespread and is detected through diverse proxies from the equatorial Atlantic Ocean (Hancock & Dickens, 2005; Bhattacharya & Dickens, 2020; D'Onofrio et al., 2020). At Site 1209 and 1210 sediments are mainly carbonate nannofossils ooze (Bralower, Premoli Silva, & Malone, 2002), so the bulk carbonate consists of mainly nannofossils and foraminifera. The CF percentage might be influenced not only by the foraminiferal contribution, but also driven by factors like dilution by bulk sediment. Besides the potential increase of calcareous nannofossil productivity and

dissolution effects, we cannot exclude that the marked morozovellid drop in abundance may have played a role in influencing the lower CF values and suggest that this should be explored further in the future.

The increased carbonate dissolution becomes more evident from the positive carbon isotope trend occurring from ~51.2 Ma close to the O Event. This interval records a shift up to +0.75‰ in Site 1209 benthic foraminiferal $\delta^{13}\text{C}$ that was initially identified in a bulk isotope record from Site 1258 by Kirtland-Turner et al. (2014) and in a benthic record at Site 1263 (Lauretano et al., 2016). It is also reported from the Tethyan Possagno and Contessa sections (Luciani et al., 2016), thus suggesting carbonate dissolution is global in scale. This positive shift has been related to the lower ocean crust production rates leading to less ^{12}C -enriched carbon released to the oceanic reservoir due to reduced CO_2 degassing (Berner et al., 1983; Bhattacharya & Dickens, 2020; Westerhold et al., 2018). The lower long-term fluxes in the exogenic carbon cycle led to less carbon input into the ocean, less carbonate leaving via seafloor deposition, with a consequent rise of carbonate saturation horizons so a rise in CCD (Bhattacharya & Dickens, 2020; Slotnick et al., 2015). Actually, during this time in the deep-sea equatorial Pacific, the carbonate saturation horizon rose significantly (Pälike et al., 2012). However, the impact of these effects is minor at Site 1209 where the CCD and lysocline were possibly deeper than those at equatorial Pacific sites and the total dissolved inorganic carbon budget remained relatively balanced as argued by Bhattacharya and Dickens (2020). The cited authors suggest that this time may record a shift in the location of carbonate accumulation and the flattening of latitudinal carbonate dissolution horizons.

Planktic foraminiferal test-size, measured for the first time here across the EECO, can be altered by physiological performance and species composition (Cooley et al., 2022; Schmidt, Thierstein, & Bollmann, 2004, 2006). Furthermore, the loss of symbionts may result in smaller size as symbiosis plays an important role in foraminiferal calcification and growth (Bé et al., 1982; Caron et al., 1982). Test-size reduction would imply an impact on carbonate burial in sediments and result in reduced CF values (e.g., Ridgwell & Zeebe, 2005). Considering the potential decrease of the symbiosis efficiency of morozovellids and given their large size recorded by semi-quantitative analysis at Atlantic sites 1051 and 1258 before the EECO onset, a test-size reduction of this group could be expected (D'Onofrio et al., 2020; Luciani et al., 2017b). The recorded test-size reduction of morozovellids is not easily linked to the parallel decrease in *Morozovella* species richness (Corfield & Granlund, 1988; D'Onofrio et al., 2020; Fraass et al., 2015; Pearson et al., 2006) as both smaller (e.g., *M. gracilis*, *M. marginodentata*) and larger species (e.g., *M. formosa*, *M. subbotinae*, *M. aequa*) gradually disappeared, and the remaining species were large (e.g., *M. aragonensis*, *M. crater*, *M. caucasica*) (e.g., D'Onofrio et al., 2020).

Contrary to expectation we observed a moderate test-size increase in the assemblage (Figure 2). In the intervals between hyperthermals before the EECO, *Morozovella* is the dominant taxon and controls size increase. With the increasing abundance of acarininids after the start of the EECO, they control size in the assemblage, especially as novel acarininid species across the EECO, such as *A. aspensis*, *A. pentacamerata* and *A. praetopilensis* are larger than their older representatives, *A. coalingenensis* and *A. wilcoxensis* (e.g., Pearson et al., 2006). To link morozovellid abundance with a potential size decrease that is associated with a reduction in symbiosis, morphometric analyses of taxa as well as automated microscopy test-size data on *Acarinina* and *Morozovella* are needed.

5. Conclusions

Our new data reveal vulnerability of some planktic foraminiferal taxa during the EECO. We found that part of the communities was not resilient and instead record profound modifications and never recover from disturbance. The main observed variation is the striking switch in the abundance of *Morozovella* (which permanently decline) compared to *Acarinina*, that proliferate from the start of the EECO. We provide support that the conditions triggering this exchange are global and happening first at equatorial latitudes and then extending to higher latitudes, possibly related to temperature gradient.

Even though the pronounced warming and associated effects permanently altered the planktic foraminiferal assemblage composition, we record substantial resilience of carbonate production in response to the EECO. The whole community was able to maintain their productivity through changes in foraminiferal assemblage composition and potentially by a change in the relative composition of foraminifers and coccolithophores. The morozovellid endurance in higher latitudes (Figure 4) or sinking to deeper waters was not enough to escape the extreme warmth of the EECO. This is possibly due to the much longer lasting EECO warmth compared to the hyperthermals (~40–200 kyr vs. ~4 My) that record resistance and recovery of planktic foraminiferal biogeochemical function across the much intense PETM warming.

The chiloguembelinids ecological niche was likely impacted by a combination of warmer thermocline temperatures, decreased food supply at depth and enhanced ODZ oxygenation that triggered their virtual disappearance after the K/X event.

Our findings highlight the importance of studying extreme warm conditions and their associated environmental changes. The recorded resilience of pelagic carbonate production needs to be considered in the context of the slow warming and the long-term steady state of the EECO and should not be directly compared to the much faster rate of anthropogenic climate change. We emphasize the need for further research to disentangle the complex interplay of temperature, ocean chemistry, nutrient availability, and other environmental factors that contribute to the observed modifications in pelagic carbonate production. This includes dedicated analyses for paleotemperature reconstruction across the sites which record the observed changes, pH reconstruction, further studies from diverse ocean settings, and test-size data for the taxa which document a shift in abundance. These future analyses will further deepen our understanding of the marine ecosystem and its responses to different climatic conditions.

Conflict of Interest

The authors declare no conflicts of interest relevant to this study.

Data Availability Statement

Planktic foraminiferal fossil record data plotted in Figures 2 and 3 can be found on Pangaea (Filippi et al., 2024) and the associated unprocessed data (including images for size-normalized weight and assemblage size analysis) can be found on the University of Bristol data repository, data.bris (Filippi, 2024). Planktic foraminiferal fossil record data plotted in Figures 2 and 3 are also available Tables S2–S5 in Supporting Information S1.

Acknowledgments

We warmly thank Simon D'haenens, Adam Woodhouse, an anonymous reviewer, and Editor Matthew Huber for the constructive comments, and the editor's assistant, Meghan Ramil, for the kind assistance and helpful evaluations during the submission and publication process. Samples were provided by the Ocean Drilling Program (ODP). We thank the Bremen Core Repository for handling our sample request. Work funded by MIUR-PRIN 2017 "Biotic Resilience to Global Change" Grant 80007370382 and FAR (Fondo Ateneo Ricerca, Ferrara University) 2023 to V.L. MIUR Grant 2018_DE_MIUR_FST_DOTTOR_sede_FG to G.F. D.N.S. was funded via NERC Grant NE/P019439/1. R.B. was funded by NERC GW4+ DTP Grant NE/S007504/1TW was funded by the Deutsche Forschungsgemeinschaft (DFG, German Research Foundation) under Germany's Excellence Strategy—EXC-2077—390741603. Open access publishing facilitated by Università degli Studi di Ferrara, as part of the Wiley - CRUI-CARE agreement.

References

- Agnini, C., Fornaciari, E., Raffi, I., Catanzariti, R., Pälke, H., Backman, J., & Rio, D. (2014). Biozonation and biochronology of Paleogene calcareous nannofossils from low and middle latitudes. *Newsletters on Stratigraphy*, 47(2), 131–181. <https://doi.org/10.1127/0078-0421/2014/0042>
- Agnini, C., Macri, P., Backman, J., Brinkhuis, H., Fornaciari, E., Giusberti, L., et al. (2009). An early Eocene carbon cycle perturbation at ~52.5 Ma in the southern alps: Chronology and biotic response. *Paleoceanography*, 24(2). <https://doi.org/10.1029/2008PA001649>
- Agnini, C., Muttoni, G., Kent, D. V., & Rio, D. (2006). Eocene biostratigraphy and magnetic stratigraphy from Possagno, Italy: The calcareous nannofossil response to climate variability. *Earth and Planetary Science Letters*, 241(3–4), 815–830. <https://doi.org/10.1016/j.epsl.2005.11.005>
- Alegret, L., Harper, D. T., Agnini, C., Newsam, C., Westerhold, T., Cramwinckel, M. J., et al. (2021). Biotic response to early Eocene warming events: Integrated record from offshore Zealandia, north Tasman Sea. *Paleoceanography and Paleoclimatology*, 36(8), e2020PA004179. <https://doi.org/10.1029/2020PA004179>
- Anagnostou, E., John, E. H., Edgar, K. M., Foster, G. L., Ridgwell, A., Inglis, G. N., et al. (2016). Changing atmospheric CO₂ concentration was the primary driver of early Cenozoic climate. *Nature*, 533(7603), 380–384. <https://doi.org/10.1038/nature17423>
- Arenillas, I., Molina, E., & Schmitz, B. (1999). Planktic foraminiferal and 13C isotopic changes across the Paleocene/Eocene boundary at Possagno (Italy). *International Journal of Earth Sciences*, 88(2), 352–364. <https://doi.org/10.1007/s005310050270>
- Auderset, A., Moretti, S., Taphorn, B., Ebner, P.-R., Kast, E., Wang, X. T., et al. (2022). Enhanced ocean oxygenation during Cenozoic warm periods. *Nature*, 609(7925), 77–82. <https://doi.org/10.1038/s41586-022-05017-0>
- Aze, T., Ezard, T. H. G., Purvis, A., Coxall, H. K., Stewart, D. R. M., Wade, B. S., & Pearson, P. N. (2011). A phylogeny of Cenozoic macroperforate planktonic foraminifera from fossil data. *Biological Reviews*, 86(4), 900–927. <https://doi.org/10.1111/j.1469-185X.2011.00178.x>
- Barrera, E., & Huber, B. T. (1991). Paleogene and early Neogene oceanography of the southern Indian Ocean: Leg 119 foraminifer stable isotope results. In J. Barron & B. Larsen (Eds.), *Proc. ODP, sci. Results, 119: College station, TX (Ocean Drilling Program)* (pp. 693–717). <https://doi.org/10.2973/odp.proc.sc.119.167.1991>
- Barrett, R., Adebowale, M., Birch, H., Wilson, J. D., & Schmidt, D. N. (2023). Planktic foraminiferal resilience to environmental change associated with the PETM. *Paleoceanography and Paleoclimatology*, 38(8), e2022PA004534. <https://doi.org/10.1029/2022PA004534>
- Bé, A. W. H., Spero, H. J., & Anderson, O. R. (1982). Effects of symbiont elimination and reinfection on the life processes of the planktonic foraminifer *Globigerinoides sacculifer*. *Marine Biology*, 70(1), 73–86. <https://doi.org/10.1007/BF00397298>
- Berger, W. H. (1970). Planktonic foraminifera: Selective solution and the lysocline. *Marine Geology*, 8(2), 111–138. [https://doi.org/10.1016/0025-3227\(70\)90001-0](https://doi.org/10.1016/0025-3227(70)90001-0)
- Berner, R. A., Lasaga, A. C., & Garrels, R. M. (1983). Carbonate-silicate geochemical cycle and its effect on atmospheric carbon dioxide over the past 100 million years. *American Journal of Science*, 283(7), 641–683. <https://doi.org/10.2475/ajs.283.7.641>
- Bhattacharya, J., & Dickens, G. R. (2020). Eocene carbonate accumulation in the north-central Pacific Ocean: New insights from Ocean Drilling Program site 1209, Shatsky rise. *Sedimentary Geology*, 405, 105705. <https://doi.org/10.1016/j.sedgeo.2020.105705>
- Boersma, A., & Premoli Silva, I. (1989). Atlantic Paleogene biserial heterohelcid foraminifera and oxygen minima. *Paleoceanography*, 4(3), 271–286. <https://doi.org/10.1029/PA004i003p00271>
- Boersma, A., Premoli Silva, I., & Shackleton, N. J. (1987). Atlantic Eocene planktonic foraminiferal paleohydrographic indicators and stable isotope paleoceanography. *Paleoceanography*, 2(3), 287–331. <https://doi.org/10.1029/PA002i003p00287>

- Bralower, T., Premoli Silva, I., Malone, M., & Thomas, D. (2002). New evidence for abrupt climate change in the Cretaceous and Paleogene: Ocean Drilling Program Leg 198 to Shatsky Rise, Northwest Pacific. *Geological Society of America Today*, *12*(11), 4–10. [https://doi.org/10.1130/1052-5173\(2002\)012<0004:NEFACC>2.0.CO;2](https://doi.org/10.1130/1052-5173(2002)012<0004:NEFACC>2.0.CO;2)
- Bralower, T. J., Premoli Silva, I., & Malone, M. (2002). Proceedings of the Ocean Drilling Program, initial reports (Vol. 198).
- Bralower, T. J., Premoli Silva, I., & Malone, M. J. (2005). Data report: Paleocene–early Oligocene calcareous nannofossil biostratigraphy, ODP Leg 198 sites 1209, 1210, and 1211 (Shatsky Rise, Pacific Ocean). *Proc. ODP, Sci. Results*, *198*, 1–15.
- Buitenhuis, E. T., Vogt, M., Moriarty, R., Bednaršek, N., Doney, S. C., Leblanc, K., et al. (2013). MAREDAT: Towards a world atlas of MARine ecosystem DATA. *Earth System Science Data*, *5*(2), 227–239. <https://doi.org/10.5194/essd-5-227-2013>
- Capdevila, P., Stott, I., Beger, M., & Salguero-Gómez, R. (2020). Towards a comparative framework of demographic resilience. *Trends in Ecology & Evolution*, *35*(9), 776–786. <https://doi.org/10.1016/j.tree.2020.05.001>
- Cappelli, C., Bown, P. R., Westerhold, T., Bohaty, S. M., de Riu, M., Lobba, V., et al. (2019). The early to middle Eocene transition: An integrated calcareous nannofossil and stable isotope record from the northwest Atlantic Ocean (integrated Ocean Drilling Program site U1410). *Paleoceanography and Paleoclimatology*, *34*(12), 1913–1930. <https://doi.org/10.1029/2019PA003686>
- Caron, D. A., Bé, A. W. H., & Anderson, O. R. (1982). Effects of variations in light intensity on life processes of the planktonic foraminifer *Globigerinoides sacculifer* in laboratory culture. *Journal of the Marine Biological Association of the United Kingdom*, *62*(2), 435–451. <https://doi.org/10.1017/S0025315400057374>
- Chaabane, S., de Garidel, T., Meilland, J., Sulpis, O., Chalk, T., Brummer, G.-J., et al. (2023). Modern planktonic Foraminifera: Migrating is not enough. *Research Square*. <https://doi.org/10.21203/rs.3.rs-3485983/v1>
- Chiu, T. C., & Broecker, W. S. (2008). Toward better paleocarbonate ion reconstructions: New insights regarding the CaCO₃ size index. *Paleoceanography*, *23*(2). <https://doi.org/10.1029/2008PA001599>
- Coffin, M. F., Frey, F. A., Wallace, P. J., & the Leg 183 Scientific Party. (2000). Leg 183 summary: Kerguelen Plateau–Broken Ridge–A large igneous province. *Proceedings of the Ocean Drilling Program: College Station, TX (Ocean Drilling Program)*, 1–101. <https://doi.org/10.2973/odp.proc.ir.183.101.2000>
- Cooley, S., Schoeman, D., Bopp, L., Boyd, P., Donner, S., Ito, S.-I., et al. (2022). Oceans and coastal ecosystems and their services. In *IPCC AR6 WGII*. Cambridge University Press.
- Corfield, R. M., & Granlund, A. H. (1988). Speciation and structural evolution in the Paleocene *Morozovella* lineage (planktonic Foraminifera). *Journal of micropaleontology*, *7*(1), 59–71.
- Davis, C. V., Shaw, J. O., D'haenens, S., Thomas, E., & Hull, P. M. (2022). Photosymbiont associations persisted in planktic foraminifera during early Eocene hyperthermals at Shatsky Rise (Pacific Ocean). *PLoS One*, *17*(9), e0267636. <https://doi.org/10.1371/journal.pone.0267636>
- De Villiers, S. (2004). Optimum growth conditions as opposed to calcite saturation as a control on the calcification rate and shell-weight of marine foraminifera. *Marine Biology*, *144*(1), 45–49. <https://doi.org/10.1007/s00227-003-1183-8>
- D'haenens, S., Bornemann, A., Roose, K., Claeys, P., & Speijer, R. (2012). Stable isotope paleoecology ($\delta^{13}\text{C}$ and $\delta^{18}\text{O}$) of early Eocene *Zeuvingerina aegyptiaca* from the north Atlantic (DSDP site 401). *Austrian Journal of Earth Sciences*, *105*(1), 179–188.
- D'Onofrio, R., Luciani, V., Dickens, G. R., Wade, B. S., & Kirtland-Turner, S. (2020). Demise of the planktic foraminifer genus *Morozovella* during the early Eocene climatic Optimum: New records from ODP site 1258 (Demerara Rise, Western equatorial Atlantic) and site 1263 (Walvis Ridge, South Atlantic). *Geosciences*, *10*(3), 88. <https://doi.org/10.3390/geosciences10030088>
- D'Onofrio, R., Luciani, V., Fornaciari, E., Giusberti, L., Galazzo, F. B., Dallanave, E., et al. (2016). Environmental perturbations at the early Eocene ETM2, H2, and I1 events as inferred by Tethyan calcareous plankton (Terche section, northeastern Italy). *Paleoceanography*, *31*(9), 1225–1247. <https://doi.org/10.1002/2016PA002940>
- Edgar, K. M., Bohaty, S. M., Gibbs, S. J., Sexton, P. F., Norris, R. D., & Wilson, P. A. (2013). Symbiont “bleaching” in planktic foraminifera during the middle Eocene climatic Optimum. *Geology*, *41*(1), 15–18. <https://doi.org/10.1130/G33388.1>
- Ernst, S. R., Guasti, E., Dupuis, C., & Speijer, R. P. (2006). Environmental perturbation in the southern Tethys across the Paleocene/Eocene boundary (Dababiya, Egypt): Foraminiferal and clay mineral records. *Marine Micropaleontology*, *60*(1), 89–111. <https://doi.org/10.1016/j.marmicro.2006.03.002>
- Filippi, G. (2024). Raw planktic foraminifera assemblage size data accompanying Filippi et al. 2024. Impacts of the Early Eocene Climatic Optimum (EECO, ~53–49 Ma) on planktic foraminiferal resilience [Dataset]. *University of Bristol*. <https://doi.org/10.5523/bris.fpl32oat0vjh25eoao7llprz3>
- Filippi, G., Barrett, R., Schmidt, D. N., D'Onofrio, R., Westerhold, T., Brombin, V., & Luciani, V. (2024). Planktic foraminiferal productivity and test-size at Pacific ODP site 198-1209 and ODP site 198-1210, Shatsky Rise, during the early Eocene climatic Optimum (EECO, ~53–49 Ma) [Dataset]. *PANGAEA*. <https://doi.org/10.1594/PANGAEA.964047>
- Filippi, G., Sigismondi, S., D'Onofrio, R., Tiepolo, M., Cannà, E., Dickens, G., et al. (2023). Planktic foraminiferal changes and the early Eocene climatic Optimum (EECO, ~53–49 Ma): Crisis or resilience strategy to global warming? (2023). Abstract. EGU General Assembly (2023), Vienna, Austria, 24–28 Apr 2023, EGU23-7934. <https://doi.org/10.5194/egusphere-egu23-7934>
- Fraass, A. J., Kelly, D. C., & Peters, S. E. (2015). Macroevolutionary history of the planktic foraminifera. *Annual Review of Earth and Planetary Sciences*, *43*(1), 139–166. <https://doi.org/10.1146/annurev-earth-060614-105059>
- Fucek, V. P., Kucenjak, M. H., & Huber, B. T. (2018). *Taxonomy, biostratigraphy, and phylogeny of Oligocene Chilouembelina and Jenkinsina*. Atlas of Oligocene Planktonic Foraminifera. Lawrence (Vol. 46, pp. 459–480). Cushman Foundation Special Publication.
- Gaskell, D. E., Huber, M., O'Brien, C. L., Inglis, G. N., Acosta, R. P., Poulsen, C. J., & Hull, P. M. (2022). The latitudinal temperature gradient and its climate dependence as inferred from foraminiferal $\delta^{18}\text{O}$ over the past 95 million years. *Proceedings of the National Academy of Sciences*, *119*(11), e2111332119. <https://doi.org/10.1073/pnas.2111332119>
- Gibbs, S. J., Bown, P. R., Murphy, B. H., Sluijs, A., Edgar, K. M., Pälike, H., et al. (2012). Scaled biotic disruption during early Eocene global warming events. *Biogeosciences*, *9*(11), 4679–4688. <https://doi.org/10.5194/bg-9-4679-2012>
- Green, O. R. (2001). *A manual of practical laboratory and field techniques in palaeobiology* (Vol. 538). Kluwer Academic.
- Guasti, E., & Speijer, R. (2007). The Paleocene-Eocene Thermal Maximum in Egypt and Jordan: An overview of the planktic foraminiferal record. *Special Papers - Geological Society of America*, *424*, 53–67.
- Hallock, P. (2000). Symbiont-bearing foraminifera: Harbingers of global change? *Micropaleontology*, *46*, 95–104.
- Hancock, H., & Dickens, G. (2005). Carbonate dissolution episodes in Paleocene and Eocene sediment, Shatsky Rise, west-central Pacific. *Proceedings of the Ocean Drilling Program - Scientific Results*, *198*, 1–24.
- Hecht, A. D. (1976). Size variations in planktonic foraminifera: Implications for quantitative Paleoclimatic analysis. *Science*, *192*(4246), 1330–1332. <https://doi.org/10.1126/science.192.4246.1330>
- Hodgson, D., McDonald, J. L., & Hosken, D. J. (2015). What do you mean, “resilient”. *Trends in Ecology & Evolution*, *30*(9), 503–506. <https://doi.org/10.1016/j.tree.2015.06.010>

- Hollis, C. J., Dunkley Jones, T., Anagnostou, E., Bijl, P. K., Cramwinckel, M. J., Cui, Y., et al. (2019). The DeepMIP contribution to PMIP4: Methodologies for selection, compilation and analysis of latest Paleocene and early Eocene climate proxy data, incorporating version 0.1 of the DeepMIP database. *Geoscientific Model Development*, 12(7), 3149–3206. <https://doi.org/10.5194/gmd-12-3149-2019>
- Hollis, C. J., Taylor, K. W. R., Handley, L., Pancost, R. D., Huber, M., Creech, J. B., et al. (2012). Early Paleogene temperature history of the Southwest Pacific Ocean: Reconciling proxies and models. *Earth and Planetary Science Letters*, 349–350, 53–66. <https://doi.org/10.1016/j.epsl.2012.06.024>
- Hönisch, B., Royer, D. L., Breecker, D. O., Polissar, P. J., Bowen, G. J., Henehan, M. J., et al. (2023). Toward a Cenozoic history of atmospheric CO₂. *Science*, 382(6675), eadi5177. <https://doi.org/10.1126/science.adi5177>
- Huber, M., & Caballero, R. (2011). The early Eocene equable climate problem revisited. *Climate of the Past*, 7(2), 603–633. <https://doi.org/10.5194/cp-7-603-2011>
- Inglis, G. N., Bragg, F., Burls, N. J., Cramwinckel, M. J., Evans, D., Foster, G. L., et al. (2020). Global mean surface temperature and climate sensitivity of the early Eocene Climatic Optimum (EECO), Paleocene–Eocene thermal maximum (PETM), and latest Paleocene. *Climate of the Past*, 16(5), 1953–1968. <https://doi.org/10.5194/cp-16-1953-2020>
- Inglis, G. N., Farnsworth, A., Lunt, D., Foster, G. L., Hollis, C. J., Pagani, M., et al. (2015). Descent toward the Icehouse: Eocene sea surface cooling inferred from GDGT distributions. *Paleoceanography and Paleoclimatology*, 30(7), 1000–1020. <https://doi.org/10.1002/2014PA002723>
- John, E. H., Pearson, P. N., Coxall, H. K., Birch, H., Wade, B. S., & Foster, G. L. (2013). Warm ocean processes and carbon cycling in the Eocene. *Philosophical Transactions of the Royal Society A: Mathematical, Physical & Engineering Sciences*, 371(2001), 20130099. <https://doi.org/10.1098/rsta.2013.0099>
- John, E. H., Wilson, J. D., Pearson, P. N., & Ridgwell, A. (2014). Temperature-dependent remineralization and carbon cycling in the warm Eocene oceans. *Palaeogeography, Palaeoclimatology, Palaeoecology*, 413, 158–166. <https://doi.org/10.1016/j.palaeo.2014.05.019>
- Keams, L. E., Bohaty, S. M., Edgar, K. M., Nogué, S., & Ezard, T. H. G. (2021). Searching for function: Reconstructing adaptive niche changes using geochemical and morphological data in planktonic foraminifera. *Frontiers in Ecology and Evolution*, 9. <https://doi.org/10.3389/fevo.2021.679722>
- Kennett, J. P. (1976). Phenotypic variation in some recent and late Cenozoic planktonic foraminifera. In R. H. Hedley & C. G. Adams (Eds.), *Foraminifera* (Vol. 2, pp. 111–170). Academic Press.
- King, D. J., & Wade, B. S. (2017). The extinction of *Chilogaembelina cubensis* in the Pacific Ocean: Implications for defining the base of the Chattian (upper Oligocene). *Newsletters on Stratigraphy*, 50(3), 311–339. <https://doi.org/10.1127/nos/2016/0308>
- Kirtland-Turner, S., Sexton, S., Charles, P., & Norriss, R. D. (2014). Persistence of carbon release events through the peak of early Eocene global warmth. *Nature Geoscience*, 7(10), 748–751. <https://doi.org/10.1038/ngeo2240>
- Knecht, N. S., Benedetti, F., Hofmann Elizondo, U., Bednaršek, N., Chaabane, S., de Weerd, C., et al. (2023). The impact of Zooplankton Calcifiers on the marine carbon cycle. *Global Biogeochemical Cycles*, 37(6), e2022GB007685. <https://doi.org/10.1029/2022GB007685>
- Kroon, D., & Nederbragt, A. J. (1990). Ecology and paleoecology of triserial planktic foraminifera. *Marine Micropaleontology*, 16(1–2), 25–38. [https://doi.org/10.1016/0377-8398\(90\)90027-J](https://doi.org/10.1016/0377-8398(90)90027-J)
- Kucera, M. (2007). Chapter Six: Planktonic foraminifera as tracers of past oceanic environments. *Developments in Marine Geology*, 1, 213–262. [https://doi.org/10.1016/S1572-5480\(07\)01011-1](https://doi.org/10.1016/S1572-5480(07)01011-1)
- Lauretano, V., Hilgen, F. J., Zachos, J. C., & Lourens, L. J. (2016). Astronomically tuned age model for the early Eocene carbon isotope events: A new high-resolution $\delta^{13}\text{C}$ benthic record of ODP site 1263 between ~49 and ~54 Ma. *Newsletters on Stratigraphy*, 49(2), 383–400. <https://doi.org/10.1127/nos/2016/0077>
- Leckie, R. M. (1987). Paleoecology of mid-Cretaceous planktonic foraminifera: A comparison of open ocean and epicontinental sea assemblages. *Micropaleontology*, 33(2), 164–176. <https://doi.org/10.2307/1485491>
- Littler, K., Röhl, U., Westerhold, T., & Zachos, J. C. (2014). A high-resolution benthic stable-isotope record for the South Atlantic: Implications for orbital-scale changes in late Paleocene–early Eocene climate and carbon cycling. *Earth and Planetary Science Letters*, 401, 18–30. <https://doi.org/10.1016/j.epsl.2014.05.054>
- Lombard, F., Erez, J., Michel, E., & Labeyrie, L. (2009). Temperature effect on respiration and photosynthesis of the symbiont-bearing planktonic foraminifera *Globigerinoides ruber*, *Orbulina universa*, and *Globigerinella siphonifera*. *Limnology & Oceanography*, 54(1), 210–218. <https://doi.org/10.4319/lo.2009.54.1.0210>
- Luciani, V., Dickens, G. R., Backman, J., Fornaciari, E., Giusberti, L., Agnini, C., & D'Onofrio, R. (2016). Major perturbations in the global carbon cycle and photosymbiont-bearing planktic foraminifera during the early Eocene. *Climate of the Past*, 12(4), 981–1007. <https://doi.org/10.5194/cp-12-981-2016>
- Luciani, V., D'Onofrio, R., Dickens, G. R., & Wade, B. S. (2017a). Did photosymbiont bleaching lead to the demise of planktic foraminifer *Morozovella* at the early Eocene climatic Optimum? Early Eocene photosymbiont bleaching. *Paleoceanography*, 32(11), 1115–1136. <https://doi.org/10.1002/2017PA003138>
- Luciani, V., D'Onofrio, R., Dickens, G. R., & Wade, B. S. (2017b). Planktic foraminiferal response to early Eocene carbon cycle perturbations in the southeast Atlantic Ocean (ODP Site 1263). *Global and Planetary Change*, 158, 119–133. <https://doi.org/10.1016/j.gloplacha.2017.09.007>
- Luciani, V., D'Onofrio, R., Dickens, G. R., & Wade, B. S. (2021). Dextral to sinistral coiling switch in planktic foraminifer *Morozovella* during the early Eocene climatic Optimum. *Global and Planetary Change*, 206, 103634. <https://doi.org/10.1016/j.gloplacha.2021.103634>
- Luciani, V., D'Onofrio, R., Filippi, G., & Moretti, S. (2020). Which was the habitat of early Eocene planktic foraminifer *Chilogaembelina*? Stable isotope paleobiology from the Atlantic Ocean and implication for paleoceanographic reconstructions. *Global and Planetary Change*, 191, 103216. <https://doi.org/10.1016/j.gloplacha.2020.103216>
- Luciani, V., & Giusberti, L. (2014). Reassessment of the early-middle Eocene planktic foraminiferal biomagnetostratigraphy: New evidence from the Tethyan Possagno section (NE Italy) and Western north Atlantic Ocean ODP site 1051. *Journal of Foraminiferal Research*, 44(2), 187–201. <https://doi.org/10.2113/gsfjr.44.2.187>
- Luciani, V., Giusberti, L., Agnini, C., Backman, J., Fornaciari, E., & Rio, D. (2007). The Paleocene–Eocene thermal maximum as recorded by Tethyan planktonic foraminifera in the Forada section (northern Italy). *Marine Micropaleontology*, 64(3), 189–214. <https://doi.org/10.1016/j.marmicro.2007.05.001>
- Molina, E., Arenillas, I., & Pardo, A. (1999). High resolution planktic foraminiferal biostratigraphy and correlation across the Palaeocene/Eocene boundary in the Tethys. *Bulletin de la Société Géologique de France*, 170(4), 521–530.
- Nederbragt, A. J. (1991). Late Cretaceous biostratigraphy and development of *Heterohellicidae* (planktic foraminifera). *Micropaleontology*, 37(4), 329–372. <https://doi.org/10.2307/1485910>

- Neukermans, G., Bach, L. T., Butterley, A., Sun, Q., Claustre, H., & Fournier, G. R. (2023). Quantitative and mechanistic understanding of the open ocean carbonate pump: Perspectives for remote sensing and autonomous in situ observation. *Earth-Science Reviews*, 239, 104359. <https://doi.org/10.1016/j.earscirev.2023.104359>
- Nguyen, T. M. P., Petrizzo, M. R., & Speijer, R. P. (2009). Experimental dissolution of a fossil foraminiferal assemblage (Paleocene–Eocene thermal maximum, Dababiya, Egypt): Implications for paleoenvironmental reconstructions. *Marine Micropaleontology*, 73(3), 241–258. <https://doi.org/10.1016/j.marmicro.2009.10.005>
- Nguyen, T. M. P., Petrizzo, M. R., Stassen, P., & Speijer, R. P. (2011). Dissolution susceptibility of Paleocene–Eocene planktic foraminifera: Implications for palaeoceanographic reconstructions. *Marine Micropaleontology*, 81(1), 1–21. <https://doi.org/10.1016/j.marmicro.2011.07.001>
- Nguyen, T. M. P., & Speijer, R. P. (2014). A new procedure to assess dissolution based on experiments on Pliocene–Quaternary foraminifera (ODP Leg 160, Eratosthenes Seamount, Eastern Mediterranean). *Marine Micropaleontology*, 106, 22–39. <https://doi.org/10.1016/j.marmicro.2013.11.004>
- Norris, R. D., Wilson, P. A., Blum, P., & Expedition, S. (2014). Paleogene Newfoundland sediment Drifts and MDHDS test. Proceedings of the Integrated Ocean Drilling Program (College Station ed.). <http://publications.iodp.org/proceedings/342/342title.htm>
- Olsson, R. K., Berggren, W. A., Hemleben, C., & Huber, B. T. (1999). Atlas of Paleocene planktonic foraminifera. *Smithsonian Contributions to Paleobiology*(85), 1–252. <https://doi.org/10.5479/si.00810266.85.1>
- Pälike, H., Lyle, M. W., Nishi, H., Raffi, I., Ridgwell, A., Gamage, K., et al. (2012). A Cenozoic record of the equatorial Pacific carbonate compensation depth. *Nature*, 488(7413), 609–614. <https://doi.org/10.1038/nature11360>
- Pearson, P. N., & Coxall, H. K. (2014). Origin of the Eocene planktonic foraminifer *Hantkenina* by gradual evolution. *Palaeontology*, 57(2), 243–267. <https://doi.org/10.1111/pala.12064>
- Pearson, P. N., Olsson, R. K., Huber, B. T., Hemleben, C., & Berggren, W. A. (2006). *Atlas of Eocene planktonic foraminifera* (Vol. 41, p. 513). Cushman Foundation Special Publication for Foraminiferal Research.
- Pearson, P. N., Shackleton, N. J., & Hall, M. A. (1993). Stable isotope paleoecology of middle Eocene planktonic foraminifera and multi-species isotope stratigraphy, DSDP Site 523, South Atlantic. *Journal of Foraminiferal Research*, 23(2), 123–140. <https://doi.org/10.2113/gsjfr.23.2.123>
- Petrizzo, M. R. (2007). The onset of the Paleocene–Eocene thermal maximum (PETM) at sites 1209 and 1210 (Shatsky rise, Pacific Ocean) as recorded by planktonic foraminifera. *Marine Micropaleontology*, 63(3–4), 187–200. <https://doi.org/10.1016/j.marmicro.2006.11.007>
- Petrizzo, M. R., Leoni, G., Speijer, R. P., De Bernardi, B., & Felletti, F. (2008). Dissolution susceptibility of some Paleogene planktonic foraminifera from ODP site 1209 (Shatsky rise, Pacific Ocean). *Journal of Foraminiferal Research*, 38(4), 357–371. <https://doi.org/10.2113/gsjfr.38.4.357>
- Premoli Silva, I., & Boersma, A. (1988). Atlantic Eocene planktonic foraminiferal historical biogeography and paleohydrographic indices. *Palaeogeography, Palaeoclimatology, Palaeoecology*, 67(3), 315–356. [https://doi.org/10.1016/0031-0182\(88\)90159-9](https://doi.org/10.1016/0031-0182(88)90159-9)
- Raffi, I., Backman, J., Zachos, J. C., & Sluijs, A. (2009). The response of calcareous nannofossil assemblages to the Paleocene Eocene thermal maximum at the Walvis ridge in the South Atlantic. *Marine Micropaleontology*, 70(3), 201–212. <https://doi.org/10.1016/j.marmicro.2008.12.005>
- Raven, J., Caldeira, K., Elderfield, H., Hoegh-Guldberg, O., Liss, P., Riebesell, U., et al. (2005). *Ocean acidification due to increasing atmospheric carbon dioxide. Policy document 12/05*. The Royal Society.
- Ridgwell, A., & Zeebe, R. E. (2005). The role of the global carbonate cycle in the regulation and evolution of the Earth system. *Earth and Planetary Science Letters*, 234(3), 299–315. <https://doi.org/10.1016/j.epsl.2005.03.006>
- Schiebel, R. (2002). Planktic foraminiferal sedimentation and the marine calcite budget. *Global Biogeochemical Cycles*, 16(4), 1–21. <https://doi.org/10.1029/2001GB001459>
- Schmidt, D. N., Lazarus, D., Young, J. R., & Kucera, M. (2006). Biogeography and evolution of body size in marine plankton. *Earth-Science Reviews*, 78(3), 239–266. <https://doi.org/10.1016/j.earscirev.2006.05.004>
- Schmidt, D. N., Renaud, S., Bollmann, J., Schiebel, R., & Thierstein, H. R. (2004). Size distribution of Holocene planktic foraminifer assemblages: Biogeography, ecology and adaptation. *Marine Micropaleontology*, 50(3–4), 319–338. [https://doi.org/10.1016/S0377-8398\(03\)00098-7](https://doi.org/10.1016/S0377-8398(03)00098-7)
- Schmidt, D. N., Thierstein, H. R., & Bollmann, J. (2004). The evolutionary history of size variation of planktic foraminiferal assemblages in the Cenozoic. *Palaeogeography, Palaeoclimatology, Palaeoecology*, 212(1), 159–180. <https://doi.org/10.1016/j.palaeo.2004.06.002>
- Schneider, L. J., Bralower, T. J., & Kump, L. R. (2011). Response of nannoplankton to early Eocene ocean deoxygenation. *Palaeogeography, Palaeoclimatology, Palaeoecology*, 310(3), 152–162. <https://doi.org/10.1016/j.palaeo.2011.06.018>
- Sexton, P. F., Wilson, P. A., & Pearson, P. N. (2006). Microstructural and geochemical perspectives on planktic foraminiferal preservation: “Glassy” versus “Frosty”. *Geochemistry, Geophysics, Geosystems*, 7(12). <https://doi.org/10.1029/2006GC001291>
- Shackleton, N. J., Corfield, R. M., & Hall, M. A. (1985). Stable isotope data and the ontogeny of Paleocene planktonic foraminifera. *Journal of Foraminiferal Research*, 15(4), 321–336. <https://doi.org/10.2113/gsjfr.15.4.321>
- Sharman, G. R., Szymanski, E., Hackworth, R. A., Kahn, A. C. M., Febo, L. A., Oefinger, J., & Gregory, G. M. (2023). Carbon isotope chemostratigraphy, geochemistry, and biostratigraphy of the Paleocene–Eocene thermal maximum, deepwater Wilcox group, Gulf of Mexico (USA). *Climate of the Past*, 19(9), 1743–1775. <https://doi.org/10.5194/cp-19-1743-2023>
- Shaw, J. O., D’haenens, S., Thomas, E., Norris, R. D., Lyman, J. A., Bornemann, A., & Hull, P. M. (2021). Photosymbiosis in planktonic foraminifera across the Paleocene–Eocene thermal maximum. *Paleobiology*, 47(4), 632–647. <https://doi.org/10.1017/pab.2021.7>
- Slotnick, B., Dickens, G., Hollis, C., Crampton, J., Percy Strong, C., & Phillips, A. (2015). The onset of the early Eocene climatic Optimum at Branch Stream, Clarence river valley, New Zealand. *New Zealand Journal of Geology and Geophysics*, 58(3), 262–280. <https://doi.org/10.1080/00288306.2015.1063514>
- Spero, H. J., & DeNiro, M. J. (1987). The influence of symbiont photosynthesis on the $\delta^{18}\text{O}$ and $\delta^{13}\text{C}$ values of planktonic foraminiferal shell calcite. *Symbiosis*, 4, 213–228.
- Spero, H. J., Lerche, I., & Williams, D. F. (1991). Opening the carbon isotope “vital effect” box. 2. Quantitative model for interpreting foraminiferal carbon isotope data. *Paleoceanography*, 6(6), 639–655. <https://doi.org/10.1029/91pa02022>
- Swain, A., Woodhouse, A., Fagan, W. F., Fraass, A. J., & Lowery, C. M. (2024). Biogeographic response of marine plankton to Cenozoic environmental changes. *Nature*, 629(8012), 616–623. <https://doi.org/10.1038/s41586-024-07337-9>
- Thunell, R. C., & Honjo, S. (1981). Calcite dissolution and the modification of planktonic foraminiferal assemblages. *Marine Micropaleontology*, 6(2), 169–182. [https://doi.org/10.1016/0377-8398\(81\)90004-9](https://doi.org/10.1016/0377-8398(81)90004-9)
- Van Hinsbergen, D. J. J., de Groot, L. V., van Schaik, S. J., Spakman, W., Bijl, P. K., Sluijs, A., et al. (2015). A paleolatitude calculator for Paleoclimate studies. *PLoS One*, 10(6), 1–21. <https://doi.org/10.1371/journal.pone.0126946>

- Wade, B. S., Pearson, P. N., Berggren, W. A., & Pälike, H. (2011). Review and revision of Cenozoic tropical planktonic foraminiferal biostratigraphy and calibration to the geomagnetic polarity and astronomical time scale. *Earth-Science Reviews*, *104*(1–3), 111–142. <https://doi.org/10.1016/j.earscirev.2010.09.003>
- Wang, Y., Cui, Y., Su, H., Jiang, J., Wang, Y., Yang, Z., et al. (2022). Response of calcareous nannoplankton to the Paleocene–Eocene thermal maximum in the Paratethys Seaway (Tarim basin, west China). *Global and Planetary Change*, *217*, 103918. <https://doi.org/10.1016/j.gloplacha.2022.103918>
- Westerhold, T., & Röhl, U. (2006). Data report: Revised composite depth records for Shatsky rise sites 1209, 1210, and 1211. *Proceedings of the Ocean Drilling Program - Scientific Results*, *198*, 1–26. <https://doi.org/10.2973/odp.proc.sr.198.122.2006>
- Westerhold, T., Röhl, U., Donner, B., & Zachos, J. C. (2018). Global extent of early Eocene hyperthermal events: A new Pacific benthic foraminiferal isotope record from Shatsky rise (ODP site 1209). *Paleoceanography and Paleoclimatology*, *33*(6), 626–642. <https://doi.org/10.1029/2017PA003306>
- Westerhold, T., Röhl, U., Frederichs, T., Agnini, C., Raffi, I., Zachos, J. C., & Wilkens, R. H. (2017). Astronomical calibration of the Ypresian timescale: Implications for seafloor spreading rates and the chaotic behavior of the solar system? *Climate of the Past*, *13*(9), 1129–1152. <https://doi.org/10.5194/cp-13-1129-2017>
- Wilson, J. D., Monteiro, F. M., Schmidt, D. N., Ward, B. A., & Ridgwell, A. (2018). Linking marine plankton ecosystems and climate: A new modeling approach to the warm early Eocene climate. *Paleoceanography and Paleoclimatology*, *33*(12), 1439–1452. <https://doi.org/10.1029/2018PA003374>
- Woodhouse, A., Jackson, S. L., Jamieson, R. A., Newton, R. J., Sexton, P. F., & Aze, T. (2021). Adaptive ecological niche migration does not negate extinction susceptibility. *Scientific Reports*, *11*(1), 15411. <https://doi.org/10.1038/s41598-021-94140-5>
- Zachos, J. C., Dickens, G. R., & Zeebe, R. E. (2008). An early Cenozoic perspective on greenhouse warming and carbon-cycle dynamics. *Nature*, *451*(7176), 279–283. <https://doi.org/10.1038/nature06588>
- Zachos, J. C., Röhl, U., Schellenberg, S. A., Sluijs, A., Hodell, D. A., Kelly, D. C., et al. (2005). Rapid Acidification of the Ocean during the Paleocene-Eocene thermal maximum. *Science*, *308*(5728), 1611–1615. <https://doi.org/10.1126/science.1109004>
- Zachos, J. C., Wara, M. W., Bohaty, S., Delaney, M. L., Petrizzo, M. R., Brill, A., et al. (2003). A transient rise in tropical Sea surface temperature during the Paleocene-Eocene thermal maximum. *Science*, *302*(5650), 1551–1554. <https://doi.org/10.1126/science.1090110>